

Outcome-guided Sparse K-means for Disease Subtype Discovery via Integrating Phenotypic Data with High-dimensional Transcriptomic Data

Lingsong Meng

University of Florida, Gainesville, USA.

Dorina Avram

University of Florida, Gainesville, USA.

George Tseng

University of Pittsburgh, Pittsburgh, USA.

and Zhiguang Huo[†]

University of Florida, Gainesville, USA.

Summary. The discovery of disease subtypes is an essential step for developing precision medicine, and disease subtyping via omics data has become a popular approach. While promising, subtypes obtained from current approaches are not necessarily associated with clinical outcomes. With the rich clinical data along with the omics data in modern epidemiology cohorts, it is urgent to develop an outcome-guided clustering algorithm to fully integrate the phenotypic data with the high-dimensional omics data. Hence, we extended a sparse K-means method to an outcome-guided sparse K-means (GuidedSparseKmeans) method, which incorporated a phenotypic variable from the clinical dataset to guide gene selections from the high-dimensional omics data. We demonstrated the superior performance of the GuidedSparseKmeans by comparing with existing clustering methods in simulations and applications of high-dimensional transcriptomic data of breast cancer and Alzheimer's disease. Our algorithm has been implemented into an R package, which is publicly available on GitHub (<https://github.com/LingsongMeng/GuidedSparseKmeans>).

Keywords: Outcome-guided clustering; sparse K-means; Disease subtype; Phenotypic data; Transcriptomic data

1. Introduction

Historically, many complex diseases were thought of as a single disease, but modern omic studies have revealed that a single disease can be heterogeneous and contain several disease subtypes. Identification of these disease subtypes is an essential step toward precision medicine, since different subtypes usually show distinct clinical responses to different treatments (Abramson et al., 2015). Disease subtyping via omics data has been prevalent in the literature, and representative diseases include leukemia (Golub et al., 1999), lymphoma (Rosenwald et al., 2002), glioblastoma (Parsons et al., 2008; Verhaak et al., 2010), breast cancer (Lehmann et al., 2011; Parker et al., 2009), colorectal cancer (Sadanandam et al., 2013), ovarian cancer (Tothill et al., 2008), Parkinson's disease (Williams-Gray and Barker, 2017) and Alzheimer's disease (Bredesen, 2015). Using breast cancer as an example, the landmark paper by Perou et al. (2000) was among the first to identify five clinically meaningful subtypes (i.e., Luminal A, Luminal B, Her2-enriched, Basal-like and Normal-like) via transcriptomic profiles, and these subtypes had shown

[†]*Address for correspondence:* Zhiguang Huo, Department of Biostatistics, University of Florida, 2004 Mowry Road, Gainesville, FL 32611-7450, USA
E-mail: zhuo@ufl.edu

distinct disease mechanisms, treatment responses and survival outcomes (Van't Veer et al., 2002). These molecular subtypes were further followed up by many clinical trial studies for the development of precision medicine (Von Minckwitz et al., 2012; Prat et al., 2015).

In the literature, many existing clustering algorithms have been successfully applied for disease subtyping, including hierarchical clustering (Eisen et al., 1998), K-means (Dudoit and Fridlyand, 2002), mixture model-based approaches, (Xie et al., 2008; McLachlan et al., 2002) and Bayesian non-parametric approaches (Qin, 2006). Due to the high dimensional nature of transcriptomic data (i.e., large number of genes and relatively small number of samples), it is generally assumed that only a small subset of intrinsic genes was relevant to disease subtypes (Parker et al., 2009). To capture these intrinsic genes and eliminate noise genes, sparse clustering methods were proposed, including sparse K-means or hierarchical clustering (Witten and Tibshirani, 2010) methods, and penalized mixture models (Pan and Shen, 2007; Wang and Zhu, 2008). In addition, due to the accumulation of multi-omics dataset (e.g., RNA-Seq, DNA methylation, copy number variation) in public data repositories, other methods (Shen et al., 2009; Wang et al., 2014; Huo et al., 2017) sought to identify disease subtypes via integrating multi-omics data.

While promising, current approaches usually only utilized the omics data for disease subtyping, and overlooked the value of the rich clinical data. It has been pointed out that the same omics data may be comprised of multi-facet clusters (Gaynor and Bair, 2017; Nowak and Tibshirani, 2008). In other words, different configurations of sample clusters defined by separated sets of genes may co-exist. For example, the desired subtype-related configuration could be driven by disease-related genes, while other configurations of clusters could be driven by sex-related genes, or other genes of unknown confounders. Without specifying disease-related genes, a sparse clustering algorithm tends to identify the configuration with the most distinct subtype patterns and separable genes, which optimizes the objective function of the algorithm. However, it is very likely that the resulting subtypes are not related to the disease, and the selected genes are not relevant to the desired biological process. Nowadays, biomedical studies usually collected comprehensive clinical information, which were quite relevant to the disease of interest and could potentially provide guidance for disease subtyping. Using breast cancer as an example, estrogen receptors (ER), progesterone receptors (PR), and human epidermal growth factor receptor 2 (HER2) are hallmarks of breast cancer, which provide mechanistic insight about the disease pathology. Incorporating such clinical information will greatly facilitate the identification of disease related subtypes and intrinsic genes, and enhance the interpretability of disease subtyping results. Therefore, it is urgent to develop a clustering algorithm to fully integrate phenotypic data with high-dimensional omics data. Hence, our goal in this paper is to develop a clinical-outcome-guided clustering algorithm.

Many statistical challenges exist to achieve this goal. (i) Only a subset of intrinsic genes is biological relevant to the disease, how to select genes that can best separate disease subtype clusters from the high dimensional data? (ii) The clinical outcome variables can be of any data type, including continuous, binary, ordinal, count, survival data, etc. How to incorporate various types of clinical outcome variables, as a guidance in determining disease subtype clusters? (iii) Since both the external clinical information and the intrinsic omics data are utilized, how to balance the contribution of them in determining the subtype clusters? (iv) How to benchmark whether the resulting subtype clusters are relevant to guidance of the clinical outcome variable? There have been some efforts in the literature to address parts of these issues. Bair and Tibshirani (2004) proposed a two-step clustering method, in which they pre-selected a list of genes based on the association strength (e.g., Cox score) with the survival outcome, and then used the selected genes to perform regular K-means. However, these pre-selected genes were purely driven by clinical outcomes, and thus might not guarantee to be good separators of the subtype clusters. Therefore, there is still lack of a unified outcome-guided clustering algorithm that can simultaneously solve all these challenges.

In this paper, we extended from the sparse K-means algorithm by Witten and Tibshirani (2010), and

proposed an outcome-guided clustering (GuidedSparseKmeans) framework which will simultaneously solve all these challenges in a unified formulation. We demonstrated the superior performance of our method in simulations as well as gene expression applications of both breast cancer and Alzheimer's disease.

2. Motivating example

To illustrate the motivation of the outcome-guided clustering (GuidedSparseKmeans) method, we used the METABRIC (Curtis et al., 2012) breast cancer gene expression data as an example, which contained 12,180 genes and 1,870 samples after preprocessing. Detailed descriptions of the METABRIC data and the preprocessing procedure are available in Section 4.2. We used the overall survival information as the clinical guidance for the GuidedSparseKmeans (namely, Survival-GuidedSparseKmeans), and compared with the non-outcome-guided method (the sparse K-means) and the two-step method (pre-select genes via Cox score, and then perform regular K-means). We used Silhouette score (Rousseeuw, 1987) to benchmark the distinction of subtype patterns of each method, for which a larger value represented both better separation between clusters and better cohesion within respective clusters. We further evaluated the association between the resulting subtypes and the overall survival to examine the biological interpretation of the subtypes of each method.

Figure 1a shows the heatmap of the subtype clustering results from the non-outcome-guided method (the sparse K-means). 408 genes (on rows) were selected and the 1,870 samples were partitioned into 5 clusters (on columns). Since the sparse K-means algorithm purely sought for a good clustering performance, it achieved the most homogeneous heatmap patterns within each subtype cluster (mean Silhouette score = 0.099). However, the resulting Kaplan-Meier survival curves (Figure 1b) of the five disease subtypes were not well-separated ($p = 0.072$), which implied that the subtype clustering results purely driven by the omics data may not necessarily be clinically meaningful.

Figure 1c shows the heatmap of the subtype clustering results from the Survival-GuidedSparseKmeans. 384 genes (on rows) were selected and the 1,870 samples were partitioned into 5 clusters (on columns). The heatmap patterns within each subtype cluster were still visually homogeneous (mean Silhouette score = 0.073). However, the GuidedSparseKmeans achieved distinct survival separation of the 5 subtype clusters ($p = 5.33 \times 10^{-10}$, Figure 1d), which was clinically meaningful. This is expected because the GuidedSparseKmeans integrated omics data with phenotypic data, seeking for simultaneous good performance in clustering and clinical relevancy.

Figure 1e shows the heatmap of the subtype clustering results from the two-step clustering method. 400 genes (on rows) were selected and the 1,870 samples were partitioned into 5 clusters (on columns). Although the marginal association two-step method achieved more distinct survival separation of the 5 subtype clusters ($p = 2.92 \times 10^{-19}$, Figure 1f), the large inter-individual variability within each subtype cluster (mean Silhouette score = 0.058) may further hamper the accurate diagnosis of the future patients.

Collectively, the sparse K-means algorithm assured homogeneous subtype clustering patterns, but the resulting subtypes might not be clinically meaningful. The two-step method encouraged the subtypes to be clinically relevant, but might result in high inter-individual variabilities within each subtype cluster. And our proposed GuidedSparseKmeans simultaneously sought for homogeneous subtype clustering patterns and relevant clinical interpretations.

3. Method

3.1. K-means and sparse K-means

3.1.1. K-means algorithm

Consider X_{gi} the gene expression value of gene $g (1 \leq g \leq G)$ and subject $i (1 \leq i \leq n)$. Throughout this manuscript, we used the gene expression data as the example to illustrate our method, which is easy

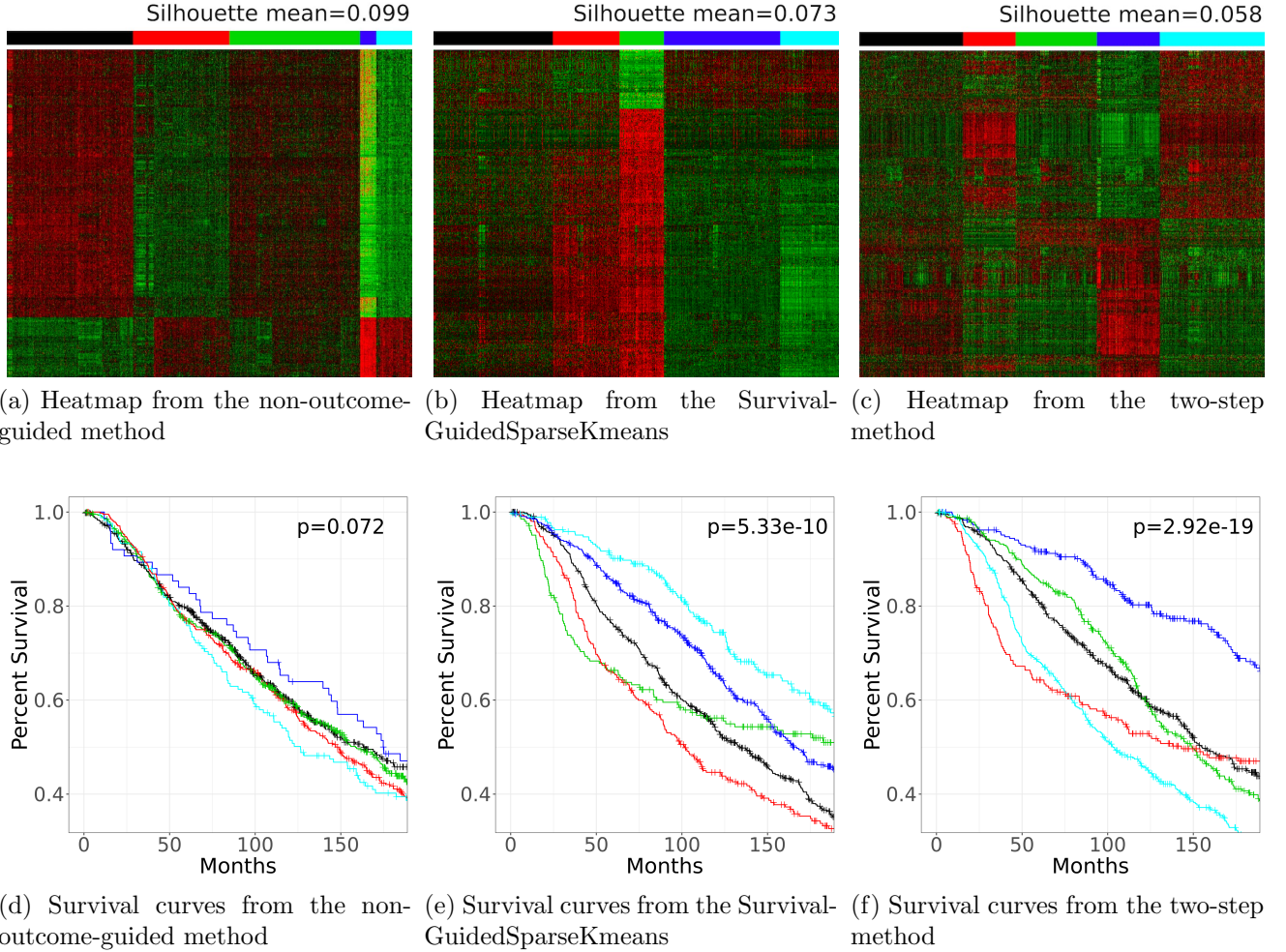


Fig. 1. Gene expression heatmap and Kaplan-Meier survival curve of the METABRIC dataset using the non-outcome-guided method (sparse K-means), the Survival-GuidedSparseKmeans, and the two-step method (pre-select genes via Cox score, and then perform regular K-means). In heatmap (a)(b)(c), rows represent genes and columns represent samples. Red color represents higher expression and green color represents lower expression. The samples are divided into 5 clusters with 5 colors in the bar above the heatmaps. In survival curves (d)(e)(f), the color of the survival curve for each subtype corresponds to the subtype color in the heatmap.

to be generalized to other types of omics data (e.g., DNA methylation, copy number variation, etc), or even non-omics data. The K-means method (MacQueen et al., 1967) aims to partition n subjects into K clusters such that the within-cluster sum of squares (WCSS) is minimized:

$$\min_C \sum_{g=1}^G WCSS_g(C) = \min_C \sum_{g=1}^G \sum_{k=1}^K \frac{1}{n_k} \sum_{i,j \in C_k} d_{ij,g}, \quad (1)$$

where C_k is a collection of indices of the subjects in cluster k ($1 \leq k \leq K$) with $C = (C_1, C_2, \dots, C_K)$; n_k is the number of subjects in cluster k ; and $d_{ij,g} = (X_{gi} - X_{gj})^2$ denotes the dissimilarity of gene g between subject i and subject j .

3.1.2. Sparse K-means algorithm

Since omics data are usually high-dimensional, with large number of genes G and relatively small number of samples n ($G \gg n$), it is generally assumed that only a small subset of intrinsic genes will contribute to the clustering result (Parker et al., 2009). To achieve gene selections in high-dimensional transcriptomic data, Witten and Tibshirani (2010) developed a sparse K-means method with lasso regularization on gene-specific weights. Since directly adding lasso regularization to Equation 1 would lead to trivial solution (i.e., all weights are 0), they instead proposed to maximize the weighted $BCSS$ (between cluster sum of square). This was because minimizing the $WCSS$ of a gene was equivalent to maximizing the $BCSS$ of the gene, as $BCSS_g(C) = TSS_g - WCSS_g(C)$ and TSS (total sum of square) is a constant for any gene. Thus the objective function of the sparse K-means algorithm is the following (Equation 2),

$$\max_{C, \mathbf{w}} \sum_{g=1}^G w_g BCSS_g(C) = \max_{C, \mathbf{w}} \sum_{g=1}^G w_g \left[\frac{1}{n} \sum_{i,j \in C} d_{ij,g} - \sum_{k=1}^K \frac{1}{n_k} \sum_{i,j \in C_k} d_{ij,g} \right] \quad (2)$$

subject to $\|\mathbf{w}\|_2 \leq 1$, $\|\mathbf{w}\|_1 \leq s$, $w_g \geq 0 \forall g$.

In Equation 2, w_g denotes the weight for gene g with $\mathbf{w} = (w_1, w_2, \dots, w_G)$; the l_1 norm penalty $\|\mathbf{w}\|_1$ will facilitate gene selection (i.e., only a small subset of genes have non-zero weights); s is a tuning parameter to control the number of nonzero weights (larger s will result in more selected genes); and the l_2 norm penalty $\|\mathbf{w}\|_2$ will encourage selecting more than one genes.

3.2. GuidedSparseKmeans

In order to incorporate the contribution from a clinical outcome variable, we proposed to use a gene specific award term U_g . U_g represents the association strength between gene g and a clinical outcome variable, which will help guide gene selections. For example, $U_g = U(\mathbf{x}_g, \mathbf{y})$, where $\mathbf{x}_g = (X_{g1}, \dots, X_{gn})^\top \in \mathbb{R}^n$ is the expression levels of gene g , and $\mathbf{y} = (y_1, \dots, y_n)^\top \in \mathbb{R}^n$ is the vector of clinical variable. The objective function of the GuidedSparseKmeans is as follows:

$$\max_{C, \mathbf{w}} \sum_{g=1}^G w_g \left[\frac{BCSS_g(C)}{TSS_g} + \lambda U_g \right] \quad (3)$$

subject to $\|\mathbf{w}\|_2 \leq 1$, $\|\mathbf{w}\|_1 \leq s$, $w_g \geq 0 \forall g$,

where λ is the tuning parameter controlling the balance between the clustering separation ability of gene g (i.e., $\frac{BCSS_g(C)}{TSS_g}$) and the guidance of the clinical variable U_g . Thus, by maximizing Equation 3, we will select genes with both strong clustering separation ability and strong association with the clinical variable.

In order to accommodate various types of clinical outcome variables, we proposed to calculate U_g based on a univariate regression model f_g . To be specific, the guiding term U_g is defined as the pseudo R-squared proposed by Cox and Snell (1989) for f_g :

$$U_g = 1 - \left[\frac{L(f_0)}{L(f_g)} \right]^{2/n}$$

where n is the number of subjects; $L(f_0)$ is the likelihood of null model; and $L(f_g)$ is the likelihood of the model f_g . Since the univariate regression model f_g can be linear models, generalized linear models, Cox models, or other regression models, the proposed U_g can accommodate a wide variety of clinical outcome variables (e.g., continuous, binary, ordinal, count, survival data, etc). We acknowledge that U_g could be also defined using the pseudo R-squared proposed by McFadden et al. (1977), Tjur (2009), Nagelkerke et al. (1991), Efron (1978) or McKelvey and Zavoina (1975), or simply the absolute value

of the Pearson correlation coefficient between \mathbf{x}_g and \mathbf{y} . $BCSS_g$ is normalized against TSS_g such that the range of $\frac{BCSS_g(C)}{TSS_g}$ is $[0, 1]$, which is comparable to the range of U_g .

To quantify whether the subtype clustering results are relevant to the clinical outcome variable, we further proposed a relevancy score by calculating the Pearson correlation of \mathbf{w}^* and \mathbf{u}^* ,

$$\text{Rel} = \text{cor}(\mathbf{w}^*, \mathbf{u}^*) \quad (4)$$

where $\mathbf{w}^* = \{w_g : w_g \neq 0\}$ and $\mathbf{u}^* = \{U_g : w_g \neq 0\}$. Since \mathbf{w}^* represents the non-zero weights of the selected genes that are associated with the clustering result, and \mathbf{u}^* is associated with the clinical outcome variable, the relevancy score indirectly quantifies the association between the subtype clustering results and the guidance of the clinical outcome variable.

REMARK 1. *The objective function of the GuidedSparseKmeans (Equation 3) will simultaneously solve all statistical challenges raised in Section 1. (i) We imposed both l_1 norm and l_2 norm penalties for the gene-specific weights, which will facilitate gene selection from the high-dimensional transcriptomic data. (ii) We proposed to use a gene-specific award term U_g to incorporate clinical information to guide the subtype clustering result. We utilized the pseudo R-squared to calculate U_g , which can accommodate all commonly encountered outcome variables, including continuous, binary, ordinal, count, survival data, etc. (iii) λ controls the balance between the separation ability of gene g (i.e., $\frac{BCSS_g(C)}{TSS_g}$) and the guidance of the clinical variable U_g , and, in Section 3.4 we proposed to use sensitivity analysis to find the optimal λ to balance these two terms. (iv) We proposed a relevancy score (Equation 4) to quantify whether the subtype clustering results are relevant to the clinical outcome variable.*

REMARK 2. *In Equation 3, λ controls the balance between the separation ability of gene g (i.e., $\frac{BCSS_g(C)}{TSS_g}$) and the guidance of the clinical variable U_g . When $\lambda = 0$, Equation 3 reduces to Equation 2. Therefore, the sparse K-means algorithm is a special case of the GuidedSparseKmeans when $\lambda = 0$. When $\lambda \rightarrow \infty$, the gene-specific weights are purely driven by the clinical outcome variable. Equation 3 reduces to the two-step clustering algorithm, and the clustering results are determined by these pre-selected genes. Therefore, the two-step algorithm is also essentially a special case of the GuidedSparseKmeans when $\lambda \rightarrow \infty$.*

3.3. Optimization

The optimization procedure is carried out as the following:

1. Denote $U_g^* = U_g \times \mathbb{I}\{U_g \geq U_{[r]}\}$, where \mathbb{I} is an indicator function and $U_{[r]}$ is the r^{th} largest element in vector $\mathbf{u} = (U_1, \dots, U_g)^\top$. We chose $r = 400$ throughout this manuscript. Initialize \mathbf{w} as $w_g = \frac{U_g^*}{\sum_{g=1}^G U_g^*} \times s$.
2. Holding \mathbf{w} fixed, update $C_k (1 \leq k \leq K)$ by weighted K-means.
3. Holding $C = (C_1, C_2, \dots, C_K)$ fixed, update \mathbf{w} as the following:

$$w_g = \frac{S(a_g, b)}{\|S(a_g, b)\|_2},$$

where S is the soft-thresholding operator defined as $S(x, c) = \max(x - c, 0)$; $a_g = \frac{BCSS_g(C)}{TSS_g} + \lambda U_g$; $b > 0$ is chosen such that $\|\mathbf{w}\|_1 = s$, otherwise, $b = 0$ if $\|\mathbf{w}\|_1 < s$.

4. Iterate Step 2-3 until the stopping rule $\frac{\|\mathbf{w}^r - \mathbf{w}^{r-1}\|_1}{\|\mathbf{w}^{r-1}\|_1} < 10^{-4}$ is satisfied, where r is the number of iterations.

In Step 2, the optimization of clusters C is essentially applying a weighted K-means algorithm on the original gene expression data, since the weights will change the relative scale of the data, and the TSS_g and λU_g are not functions of C . In Step 3, fixing the clusters C , the optimization of weights \mathbf{w} is a convex problem, and a closed form solution of \mathbf{w} can be derived by Karush-Kuhn-Tucker (KKT) conditions (Boyd and Vandenberghe, 2004; Witten and Tibshirani, 2010).

3.4. Selection of tuning parameter

The GuidedSparseKmeans objective function (Equation 3) has three tuning parameters: K is the number of clusters; s controls the number of selected genes; and λ controls the balance between the clustering separation ability and the guidance from the clinical outcome. Below are our guidelines on how to select these tuning parameters.

3.4.1. Selection of K

How to select number of clusters K has been widely discussed in the literature (Milligan and Cooper, 1985; Kaufman and Rousseeuw, 2009; Sugar and James, 2003; Tibshirani and Walther, 2005; Tibshirani et al., 2001). Here, we suggested K to be estimated using the gap statistics (Tibshirani et al., 2001) or prediction strength (Tibshirani and Walther, 2005). Alternatively, K can be set as a specific number in concordance with the prior knowledge of the disease. In our simulation, we selected top N genes (e.g., $N = 400$) with the largest U_g 's, and used gap statistics to select K based on the N pre-selected genes. As shown in Figure 2a, the gap statistics successfully identified $K = 3$ as the optimal number of clusters, which had the largest gap statistics.

3.4.2. Selection of λ

λ controls the balance between the separation ability of gene g (i.e., $\frac{BCSS_g(C)}{TSS_g}$) and the guidance of the clinical variable U_g . We recommend to use sensitivity analysis to select λ . When $\lambda \rightarrow \infty$, the selected genes as well as the clustering results are purely driven by the guidance of the clinical variable U_g . As λ gradually decreases, we expect stable results of gene selection and clustering results, until a certain transition point. After the transition point, we expect the separation ability $\frac{BCSS_g(C)}{TSS_g}$ becomes dominant, and both gene selection and clustering results may change. Therefore, our rationale is to identify the transition point λ^* , which is the smallest λ such that the clustering results and the gene selection results are stable with respect to any $\lambda \geq \lambda^*$. Below is the detailed algorithm:

1. Let $\lambda^M = (\lambda_1, \dots, \lambda_m, \dots, \lambda_M)$, $\lambda_m = 0.25m$ for $1 \leq m \leq M$. Obtain the clustering result $C(\lambda_m, s, K)$ and gene weight $\mathbf{w}(\lambda_m, s, K)$ for each λ_m ($1 \leq m \leq M$) by applying the GuidedSparseKmeans, where K is pre-estimated, and s is pre-set so that q genes can be selected by the GuidedSparseKmeans (q is recommended to set between 200 and 800). We set $M = 10$ throughout this paper. Since both s and K are fixed, we use $C(\lambda_m)$ to denote $C(\lambda_m, s, K)$, and $\mathbf{w}(\lambda_m)$ to denote $\mathbf{w}(\lambda_m, s, K)$. For $1 \leq m \leq M - 1$, we further calculate the adjusted Rand index (Hubert and Arabie, 1985) (ARI) between $C(\lambda_m)$ and $C(\lambda_{m+1})$ as $A(m, m + 1)$. Similarly, we calculate the Jaccard index (Jaccard, 1901) between $\mathbb{I}\{\mathbf{w}(\lambda_m) = 0\}$ and $\mathbb{I}\{\mathbf{w}(\lambda_{m+1}) = 0\}$ as $J(m, m + 1)$, where \mathbb{I} is an indicator function. ARI measures the agreement of two clustering results, and the Jaccard index measures the agreement of two gene sets (see Section 4 for details).
2. For $2 \leq m \leq M - 2$, calculate $\mu_A(m) = \frac{1}{M-m} \sum_{i=m}^{M-1} A(i, i + 1)$; $\sigma_A(m)$ as the standard deviation of $A(i, i + 1)$'s for $m \leq i \leq M - 1$; $\mu_J(m) = \frac{1}{M-m} \sum_{i=m}^{M-1} J(i, i + 1)$; and $\sigma_J(m)$ as the standard deviation of $J(i, i + 1)$'s for $m \leq i \leq M - 1$.

3. We calculate m^{A*} as the largest m such that $A(m-1, m) < \mu_A(m) - 2 \max\{\sigma_A(m), \delta\}$, where we set the fudge parameter $\delta = 0.05$ to avoid the zero variation. Similarly, we calculate m^{J*} as the largest m such that $J(m-1, m) < \mu_J(m) - 2 \max\{\sigma_J(m), \delta\}$. m^{A*} and m^{J*} mimic the transition points for the clustering result and gene selection result, respectively.
4. We select λ as $\lambda^* = \max\{\lambda_{m^{A*}}, \lambda_{m^{J*}}\}$
5. If $A(m, m+1)$ (or $J(m, m+1)$) is very stable for all $1 \leq m \leq M-1$, it is possible that m^{A*} (or m^{J*}) will not be obtained. Under this scenario, λ is not sensitive to clustering (or gene selection result). Since $\lambda^* = \max\{\lambda_{m^{A*}}, \lambda_{m^{J*}}\}$, we will set $m^{A*} = 1$ (or $m^{J*} = 1$) to let its alternative component m^{J*} (or m^{A*}) to decide the proper λ .

Based on the above algorithm, the clustering results and gene selection results will not be sensitive to λ if $\lambda \geq \lambda^*$. We applied this sensitivity analysis algorithm to select λ for a simulated data that is introduced in Section 4.1. Figure 2c shows the value of $A(m, m+1)$ for each m ($1 \leq m \leq 9$) and Figure 2d shows the value of $J(m, m+1)$ for each m ($1 \leq m \leq 9$). $\lambda_{m^{A*}} = 0.25$ ($m^{A*} = 1$) and $\lambda_{m^{J*}} = 1.5$ ($m^{J*} = 6$) were obtained. Therefore, we will set $\lambda^* = 1.5$ in this specific simulation via sensitivity analysis.

3.4.3. Selection of s

After K and λ are selected, we extend the gap statistics procedure in the sparse K-means (Witten and Tibshirani, 2010) to estimate s , which controls the number of selected genes:

1. Pre-specify a set of candidate tuning parameter s .
2. Create B permuted datasets $X^{(1)}, X^{(2)}, \dots, X^{(B)}$ by randomly permuting subjects for each gene feature of the observed data X .
3. Compute the gap statistics for each candidate tuning parameter s as the following:

$$Gap(s) = O(s) - \frac{1}{B} \sum_{b=1}^B O_b(s)$$

where $O(s) = \log(\sum_{g=1}^G w_g^* BCSS_g(C^*))$ is the log weighted $BCSS$ value on the observed data X with w_g^* , C^* being the optimum solution. Similarly, $O_b(s)$ is the log weighted $BCSS$ value on the permuted data $X^{(b)}$ and their corresponding optimum solutions.

4. Choose s^* such that the $Gap(s^*)$ is maximized.

We applied the gap statistics algorithm to select s for the simulated data mentioned in the selection of K . Figure 2b shows the gap statistics for each candidate s ($s = 11, 11.5, \dots, 15$). s^* was chosen to be 13.5 and the number of selected genes is 370, which is close to the underlying truth (389 intrinsic genes).

4. Result

We evaluated the performance of the GuidedSparseKmeans on simulation datasets and two gene expression profiles of breast cancer and Alzheimer's disease, and compared with the non-outcome-guided method (the sparse K-means) and the two-step clustering method (regular K-means with pre-selected genes via Cox score). We used the adjusted Rand index (Hubert and Arabie, 1985) (ARI) to benchmark the clustering performance, which evaluates the similarity between a clustering result and the

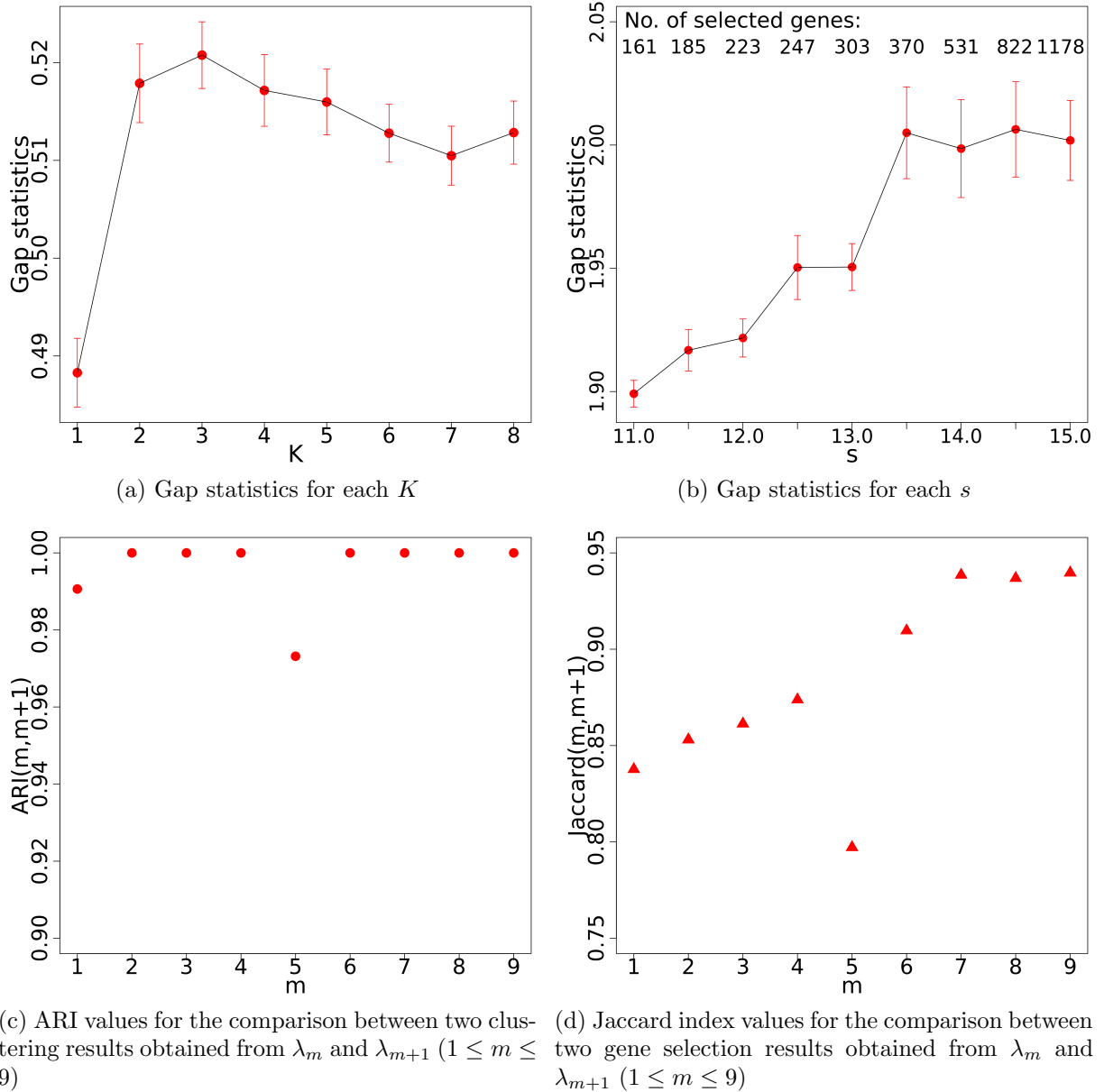


Fig. 2. Selection of tuning parameters in a simulated dataset with biological variation $\sigma_1 = 3$. Figure 2(a): Gap statistics to select K . Gap statistics is maximized at $K = 3$. Figure 2(b): Gap statistics to select s . The number of selected genes corresponding to each candidate s is showed on the top. Gap statistics is maximized at $s = 13.5$, which is corresponding to 370 genes. Figure 2(c)(d): Sensitivity analysis to select λ . The values of $A(m, m+1)$ and $J(m, m+1)$ are calculated for each m . $m^{A*} = 1$ and $m^{J*} = 6$ are transition points in (c) and (d) respectively. The estimated λ^* is 1.5 ($\max\{\lambda_{m^{A*}}, \lambda_{m^{J*}}\}$).

underlying truth (ranges from 0 [random agreement] to 1 [perfect agreement]). We used the Jaccard index (Jaccard, 1901) to benchmark the similarity of the selected genes to the underlying intrinsic genes, which is defined as the ratio of the number of genes from both gene sets to the number of genes from either one of the gene sets (ranges from 0 [no intersection between the two gene sets] to 1 [identical gene sets]).

4.1. Simulation

4.1.1. Simulation setting

To evaluate the performance of the GuidedSparseKmeans and to compare with the non-outcome-guided method (the sparse K-means), we simulated a study with $K = 3$ subtypes. To best preserve the nature of genomic data, we simulated intrinsic genes (i.e., genes defining subtype clusters), confounding impacted genes (i.e., genes defining other configurations of clusters), and noise genes with correlated gene structures (Song and Tseng, 2014; Huo et al., 2016). In addition, we generated a continuous outcome variable as the clinical guidance. Below is the detailed data generative process.

(a) Intrinsic genes.

1. Simulate $N_k \sim POI(100)$ subjects for subtype $k (1 \leq k \leq K)$ and the number of subjects in the study is $N = \sum_k N_k$.
2. Simulate $M = 20$ gene modules ($1 \leq m \leq M$). Denote n_m as the number of features in module $m (1 \leq m \leq M)$. In each module, sample the number of genes n_m by $n_m \sim POI(20)$. Therefore, there will be an average of 400 intrinsic genes.
3. Denote θ_k as the baseline gene expression of subtype $k (1 \leq k \leq K)$ of the study and $\theta_k = 2 + 2k$. Denote μ_{km} as the template gene expression of subtype k and module $m (1 \leq m \leq 20)$. We calculate the template gene expression by $\mu_{km} = \alpha_m \theta_k + N(0, \sigma_0^2)$, where α_m is the fold change for each module m and $\alpha_m \sim UNIF((-2, -0.2) \cup (0.2, 2))$. σ_0 is set to be 1.
4. Add biological variation σ_1^2 to the template gene expression and generate $X'_{kmi} \sim N(\mu_{km}, \sigma_1^2)$ for each module $m (1 \leq m \leq 20)$, subject $i (1 \leq i \leq N_k)$ of subtype k . σ_1 is set to be 3 unless otherwise specified.
5. Simulate the covariance matrix Σ_{km} for genes in subtype k and module $m (1 \leq m \leq 20)$. First sample $\Sigma'_{km} \sim W^{-1}(\phi, 60)$, where $\phi = 0.5I_{n_m \times n_m} + 0.5J_{n_m \times n_m}$, W^{-1} denotes the inverse Wishart distribution, I is the identity matrix and J is the matrix with all elements equal to 1. The Σ_{km} is calculated by standardizing Σ'_{km} such that all the diagonal elements are equal to 1.
6. Simulate gene expression values for subject i in subtype k and module m as $(X_{1kmi}, \dots, X_{n_m kmi})^\top \sim MVN(X'_{kmi}, \Sigma_{km})$, where $1 \leq k \leq 3$, $1 \leq m \leq 20$ and $1 \leq i \leq N_k$.

(b) Phenotypic variables.

1. Simulate clinical outcomes as $Y_{ki} \sim N(\theta_k, \sigma_2^2)$ for subject i and in subtype k , where $1 \leq i \leq N_k$ and $1 \leq k \leq 3$. σ_2 is set to be 8 such that the magnitude of U_g of the intrinsic genes in this simulation is similar to the breast cancer example (Section 4.2).

(c) Confounding impacted genes.

1. Simulate $C = 4$ confounding variables. Confounding variables can be demographic factors such as race, gender, or other unknown confounding variables. These variables will define other configurations of sample clustering patterns, and thus complicate disease subtype discovery. For each confounding variable $c (1 \leq c \leq C)$, we simulate $R = 20$ modules. For each module $r_c (1 \leq r_c \leq R)$, sample number of genes $n_{rc} \sim POI(20)$. Therefore, there will be an average of 1,600 confounding impacted genes.
2. For each confounding variable c in the study, the N samples are randomly divided into K subclasses, which represents the configuration of clusters for confounding variables.
3. Similar to Step a3, we denote θ_k as the baseline gene expression of subclass $k (1 \leq k \leq K)$ for each confounding variable, and set $\theta_k = 2 + 2k$. Denote μ_{kr_c} as the template gene expression in subclass $k (1 \leq k \leq K)$ and module $r_c (1 \leq r_c \leq 20)$. We calculate the template gene

Table 1. Comparison in the performance of clustering and gene selection between the GuidedSparseKmeans and the sparse K-means with biological variation $\sigma_1 = 3$. Mean estimates and standard errors were reported based on $B = 100$ simulations. Clustering accuracy were evaluated by ARI. Gene selection accuracy were evaluated by Jaccard index and AUC.

	Clustering results		Gene selection results	
	ARI	Jaccard index	AUC	
GuidedSparseKmeans	0.730 (0.017)	0.728 (0.016)	0.881 (0.008)	
sparse K-means	0.178 (0.018)	0.179 (0.018)	0.590 (0.010)	

expression by $\mu_{kr_c} = \alpha_{r_c}\theta_k + N(0, \sigma_0^2)$, where α_{r_c} is the fold change for each module r_c and $\alpha_{r_c} \sim UNIF((-2, -0.2) \cup (0.2, 2))$.

4. Add biological variation σ_1^2 to the template gene expression and generate $X'_{kr_c i} \sim N(\mu_{kr_c}, \sigma_1^2)$. Similar to Step a5 and a6, we simulate gene correlation structure within modules of confounder impacted genes.

(d) Noise genes.

1. Simulate 8,000 noninformative noise genes denoted by g . We generate template gene expression $\mu_g \sim UNIF(4, 8)$. Then, we add noise $\sigma_3 = 1$ to the template gene expression and generate $X_{gi} \sim N(\mu_g, \sigma_3^2)$.

4.1.2. Simulation results

In this section we compared the performance of the GuidedSparseKmeans and the non-outcome-guided algorithm (sparse K-means algorithm). For the GuidedSparseKmeans, the guidance term U_g was calculated as the R^2 from univariate linear regressions. The number of clusters was estimated as $K = 3$ via the gap statistics in Section 3.4.1. The tuning parameter λ for the GuidedSparseKmeans for each single simulation was selected based on sensitivity analysis (See Section 3.4.2 for details). For a fair comparison, we selected the tuning parameter s such that the numbers of genes selected using the GuidedSparseKmeans and the sparse K-means were close to the number of intrinsic genes in each simulation (i.e., 400).

Table 1 shows the comparison results of two methods with the biological variation $\sigma_1 = 3$. The GuidedSparseKmeans (mean ARI = 0.730) outperformed the sparse K-means (mean ARI = 0.178) in terms of clustering accuracy. In addition, in terms of gene selection, the GuidedSparseKmeans (mean Jaccard index = 0.728) outperformed the sparse K-means (mean Jaccard index = 0.179). To ensure the performance difference between the two methods was due to methodology itself instead of the tuning parameter selection, we further compared the gene selection performance in terms of the area under the curve (AUC) of a ROC curve, which aggregated the performance of all candidate tuning parameter s 's. And not surprisingly, the GuidedSparseKmeans (mean AUC = 0.881) achieved better performance than the sparse K-means (mean AUC = 0.590). Further, under the settings with varying biological variation ($\sigma_1 = 1$ to 5 with interval 0.25), Figure 3a and Figure 3b show that the GuidedSparseKmeans still outperformed the sparse K-means algorithm in terms of both clustering and gene selection accuracy, though the performance of both methods decreased as the biological variation increased.

4.2. METABRIC breast cancer example

In this section, we evaluated the performance of the GuidedSparseKmeans in the METABRIC breast cancer gene expression dataset (Curtis et al., 2012), which included samples from tumor banks in the UK and Canada. The METABRIC cohort contains gene expression profile of 24,368 genes and 1,981

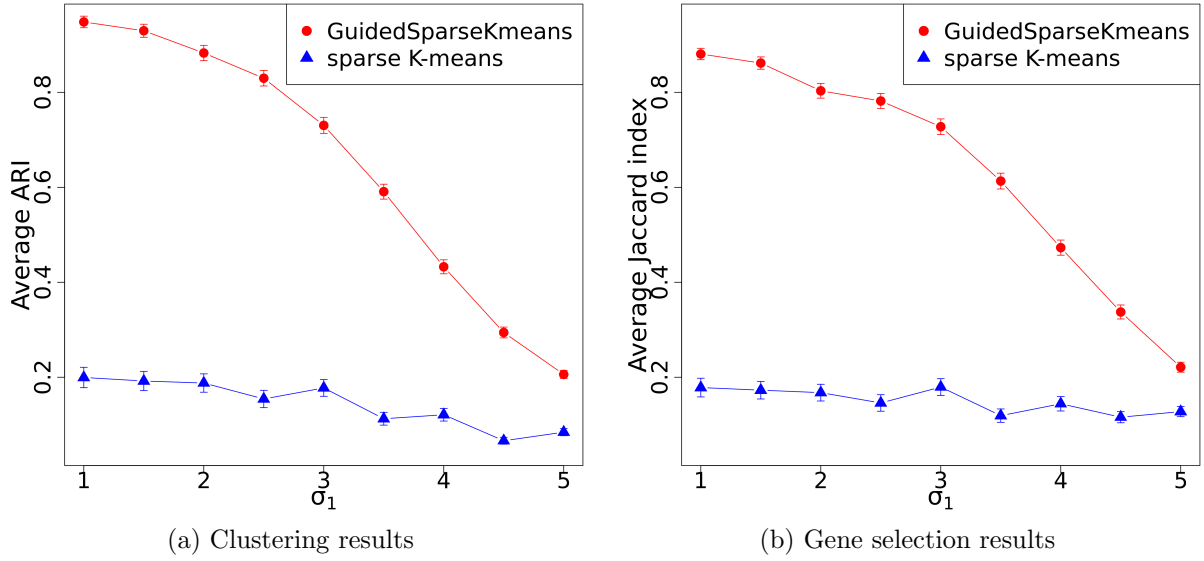


Fig. 3. Simulation results for the comparison between the GuidedSparseKmeans and the sparse K-means with different values of biological variation σ_1 . Mean estimates and standard errors were reported based on $B = 100$ simulations. Figure 3(a): Clustering accuracy were evaluated using ARI. Figure 3(b): Gene selection accuracy were evaluated using Jaccard index.

subjects, as well as various types of clinical outcome variables including the Nottingham prognostic index (NPI, continuous variable); Estrogen receptor status (ER, binary variable); HER2 receptor status (HER2, ordinal variable); and overall survival. We used each of these 4 phenotypic variables as the clinical guidance for the GuidedSparseKmeans, respectively. All datasets are publicly available at <https://www.cbioportal.org>. We matched the gene expression data to the clinical data by removing missing samples. After filtering out 50% low expression genes based on the average expression level of each gene, we scaled the data such that each gene has mean expression value 0 and standard deviation 1. After these preprocessing procedures, we ended up with 12,180 gene features and 1,870 subjects.

For each of these outcome variables, we calculated U_g as the R^2 or pseudo- R^2 from the univariate regression between gene g and an outcome variable, where we used the linear model for continuous outcomes; generalized linear models for binary and ordinal outcomes; and the Cox regression model for survival outcomes. We set the tuning parameter $K = 5$ since it was well acknowledged that there are 5 types of breast cancer by the PAM50 definition (Parker et al., 2009). The tuning parameter λ of GuidedSparseKmeans was selected automatically (See methods in Section 3.4.2). To compare with other methods fairly, we selected the tuning parameter s such that the number of selected genes was closest to 400. To benchmark the performance of the GuidedSparseKmeans, we further compared with the non-outcome-guided clustering algorithm (the sparse K-means) and the two-step clustering method, with number of selected genes around 400 (See Table 2).

4.2.1. Evaluating the clustering performance

Since we did not have the underlying true clustering result, we used the survival difference between subtypes to examine whether the resulting subtypes were clinically meaningful. As shown in Figure 1, Figure 4, and Table 2, the Kaplan-Meier survival curves of the five disease subtypes obtained from each GuidedSparseKmeans method or the two-step method were well separated with significant p-values, but not for the non-outcome-guided method (the sparse K-means). This is not unexpected

Table 2. Comparison in clustering and gene selection of the four GuidedSparseKmeans methods, the sparse K-means method, and the two-step method. The number of genes selected by each method was close to 400. The relevancy of the subtype clustering result and the clinical outcome variable was evaluated by the relevancy score. The clustering results were compared with PAM50 subtype in terms of ARI. The separation between resulting clusters and cohesion in respective clusters were evaluated by the Silhouette score. P-values of survival differences of identified subgroups were calculated based on log-rank test.

Method	Guidance	Genes	Relevancy	ARI	Silhouette	p-value	Time
Guided SparseKmeans	NPI(continuous)	399	0.690	0.237	0.065	6.25×10^{-8}	31 secs
	ER(binary)	411	0.764	0.292	0.093	1.64×10^{-10}	3.3 mins
	HER2(ordinal)	394	0.305	0.292	0.108	1.62×10^{-13}	19.2 mins
	Survival	384	0.559	0.244	0.073	5.33×10^{-10}	2.9 mins
sparse K-means		408		0.017	0.099	0.072	9.8 mins
two-step method	Survival	400		0.177	0.058	2.92×10^{-19}	2.5 mins

because except for the sparse K-means method, all the other methods have guidance from clinical outcomes. Remarkable, even though the NPI-GuidedSparseKmeans, the ER-GuidedSparseKmeans, and the HER2-GuidedSparseKmeans did not utilize any survival information, they still achieved good survival separation. Probable reason could be that these clinical variables were all related to the disease, and thus could impact the overall survival.

We further compared the clustering results obtained from each method with PAM50 subtypes, which were considered as the gold standard for breast cancer subtypes. Table 2 shows that the ARI values from four types of GuidedSparseKmeans ($0.237 \sim 0.292$) were greater than the ARI values from the sparse K-means (0.017) or the two-step method (0.177), indicating that the subtype results from the GuidedSparseKmeans were closer to the gold standard than those from the sparse K-means or the two-step method.

For the heatmap patterns, in general the sparse K-means achieved the most homogenous clustering results (mean Silhouette = 0.099), followed by the GuidedSparseKmeans (mean Silhouette = 0.065 \sim 0.108), and the two-step method achieved the most heterogenous clustering results (mean Silhouette = 0.058). Notably, the HER2-GuidedSparseKmeans achieved even better mean Silhouette score than the sparse K-means (mean Silhouette = 0.108).

To examine whether the subtype clusters from the GuidedSparseKmeans were relevant to the guidance of the clinical variables, we calculated the relevancy score by Equation 4. The ER-GuidedSparseKmeans achieved the highest relevancy score (0.764), followed by NPI guided sparse K-means (0.690), Survival guided sparse K-means (0.559), and HER2 guided sparse K-means (0.305) indicating the clustering results from all GuidedSparseKmeans methods reasonably reflected the information of their clinical outcomes.

Collectively, as discussed in the motivating example, the sparse K-means algorithm only sought for homogeneous subtype clustering patterns, regardless of whether the resulting subtypes were clinically meaningful. The two-step method only sought for subtypes that were clinically meaningful, which could result in high inter-individual variabilities within each subtype cluster. And the GuidedSparseKmeans sought for both homogeneous subtype clustering patterns and relevant clinical interpretations.

4.2.2. Evaluating the gene selection performance

To evaluate whether the selected genes were biologically meaningful, we performed pathway enrichment analysis via the BioCarta pathway database using the Fisher's exact test. Figure 5 shows the jitter plot of p-values for all pathways obtained from each method. Using $p = 0.05$ as significance cutoff, the points above the black horizon line are the significantly enriched pathways without correcting for multiple comparisons. We observed that the genes selected from the GuidedSparseKmeans (number of significant

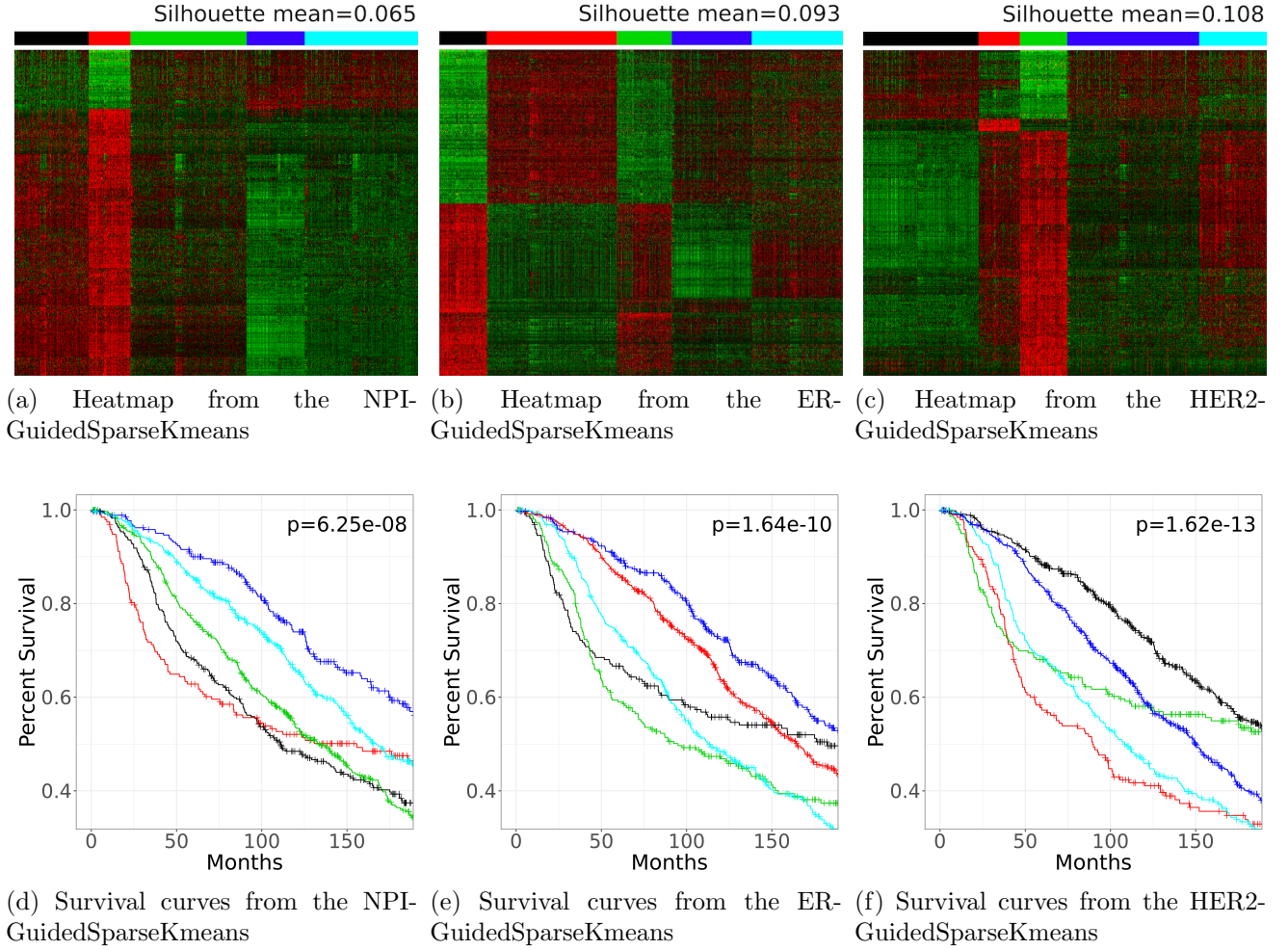


Fig. 4. Gene expression heatmap and Kaplan–Meier survival curve of the METABRIC dataset using the NPI-GuidedSparseKmeans, the ER-GuidedSparseKmeans and the HER2-GuidedSparseKmeans. In heatmap (a)(b)(c), rows represent genes and columns represent samples. Red color represents higher expression and green color represents lower expression. The samples are divided into 5 clusters with 5 colors in the bar above the heatmaps. In survival curves (d)(e)(f), the color of the survival curve for each subtype is corresponding to the subtype color in the heatmap.

pathways = 7 ~ 10) and the two-step method (number of significant pathways = 9) had better biological interpretation than the sparse K-means method (number of significant pathways = 4). Also, the top p-values from the GuidedSparseKmeans were more significant than those from the two-step method. Notably, the genes selected by the ER-GuidedSparseKmeans and the HER2-GuidedSparseKmeans were enriched in HER2 pathway, with $p = 5.78 \times 10^{-3}$ and 5.14×10^{-3} , respectively. This is in line with previous research that ER signaling pathway and HER2 signaling pathway are closely related to breast cancer (Giuliano et al., 2013). In addition, all GuidedSparseKmeans methods identified ATRBRCA pathway as significant, which has been found closely related to breast cancer susceptibility (Paul and Paul, 2014). However, these hallmark pathways of breast cancer were not picked up by the sparse K-means algorithm or the two-step method, and only the GuidedSparseKmeans selected the most biologically interpretable genes.

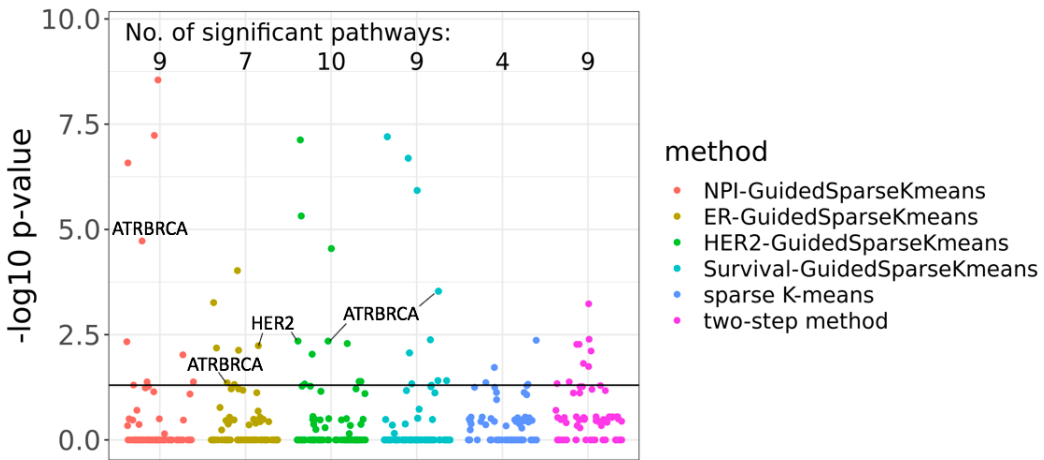


Fig. 5. Pathway enrichment analysis results for the GuidedSparseKmeans with four different types of guidance, the sparse K-means, and the two-step method. The number of significant pathways ($p < 0.05$) for each method is on the top.

4.2.3. Evaluating the computing time

The computing time for the GuidedSparseKmeans in this real application was 31 seconds for continuous outcome guidance, 2.9 minutes for survival outcome guidance, 3.3 minutes for binary outcome guidance, and 19.2 minutes for ordinal outcome guidance. Since our high-dimensional expression data contains 12,180 genes and 1,870 samples, such computing time is reasonable and applicable in large transcriptomic applications.

In general, the computing time of our method was faster than the sparse K-means method (9.8 minutes), except for the ordinal outcome guidance. This was because we used U_g to guide the initialization of the weights instead of equal weight initialization in the sparse K-means, which saved lots of time in the first step weighted K-means iteration. The ordinal outcome GuidedSparseKmeans was slow, because of the slow fitting of ordinal logistic regression models. Our methods were generally slower than the two-step method, except for the continuous outcome guidance. This was because the two-step method only needed to update the clustering assignment once, while ours needed to iteratively update the clustering assignment and gene weight. The continuous-outcome-GuidedSparseKmeans was super-fast (31 seconds), because the R^2 of univariate linear models can be efficiently calculated as the square of the Pearson correlation between a gene and the outcome variable.

4.3. Alzheimer disease example

In this section, we applied the sparse K-means and the GuidedSparseKmeans to an RNA-seq dataset of Alzheimer disease (AD). AD is a devastating neurodegenerative disorder affecting elder adults, with neurofibrillary tangles and neuritic plaques as disease hallmarks. The dataset we used included 30,727 transcripts from post mortem fusiform gyrus tissues of 217 AD subjects, which is available at <https://www.ncbi.nlm.nih.gov> under GEO ID GSE125583. After normalizing the gene expression data, filtering out 50% low expression genes based on the average expression level of each gene, and scaling each gene to mean 0 and standardization 1, we ended up with 15,363 gene features. We utilized the Braak stage as the clinical outcome variable, which is a semiquantitative measure of severity of neurofibrillary tangles (Braak and Braak, 1991). Since the Braak system has 6 stages (1 ~ 6), we treated it as a continuous variable, and calculated U_g as the R^2 from the univariate linear regression between gene g and the Braak stage. We set the tuning parameter $K = 6$ to be consistent with the number of Braak

stages. The tuning parameter λ of GuidedSparseKmeans was selected automatically using the method in Section 3.4.2. The tuning parameter s was selected such that the number of selected genes was closest to 400. The computing time for this example was only 7 seconds. Also, the sparse K-means was applied to obtain about 400 genes and the computing time was 22 seconds.

The resulting heatmap of the selected genes from the sparse K-means and the GuidedSparseKmeans in Figure 6 showed a gradient effect from left (green color, lower level of expression) to right (red color, higher level of expression). We labeled the clusters using the integers 1 to 6 which corresponds to the gene expression level from low to high. To evaluate whether the resulting AD subtypes were biologically meaningful, we calculated the Pearson correlation between the subtype labels and the Braak stages. The correlation coefficients were 0.056 and 0.282 for the sparse K-means and the GuidedSparseKmeans respectively, indicating that the AD subtypes obtained by the GuidedSparseKmeans were more related to neurofibrillary tangles, a key hallmark of AD, than those obtained by the sparse K-means.

To examine whether clusters from the GuidedSparseKmeans were relevant to the guidance of the clinical variable Braak staging, we calculated the relevancy score by Equation 4. The relevancy score was 0.309, indicating the GuidedSparseKmeans reflected the information of the clinical outcome. To further examine whether the genes selected from the GuidedSparseKmeans were biologically meaningful, we performed pathway enrichment analysis via the BioCarta pathway database using the Fisher's exact test. Notably, the genes selected by the Braak-GuidedSparseKmeans were enriched in GPCR signaling pathway ($p = 6.59 \times 10^{-6}$) and NOS1 signaling pathway ($p = 1.61 \times 10^{-5}$), both of which were involved in the neuropathological processes of AD (Zhao et al., 2016; Reif et al., 2011). However, these hallmark pathways were not picked up by the sparse K-means method. Therefore, compared with the sparse K-means, the GuidedSparseKmeans successfully identified AD subtypes and the intrinsic genes that were both closely related to AD.

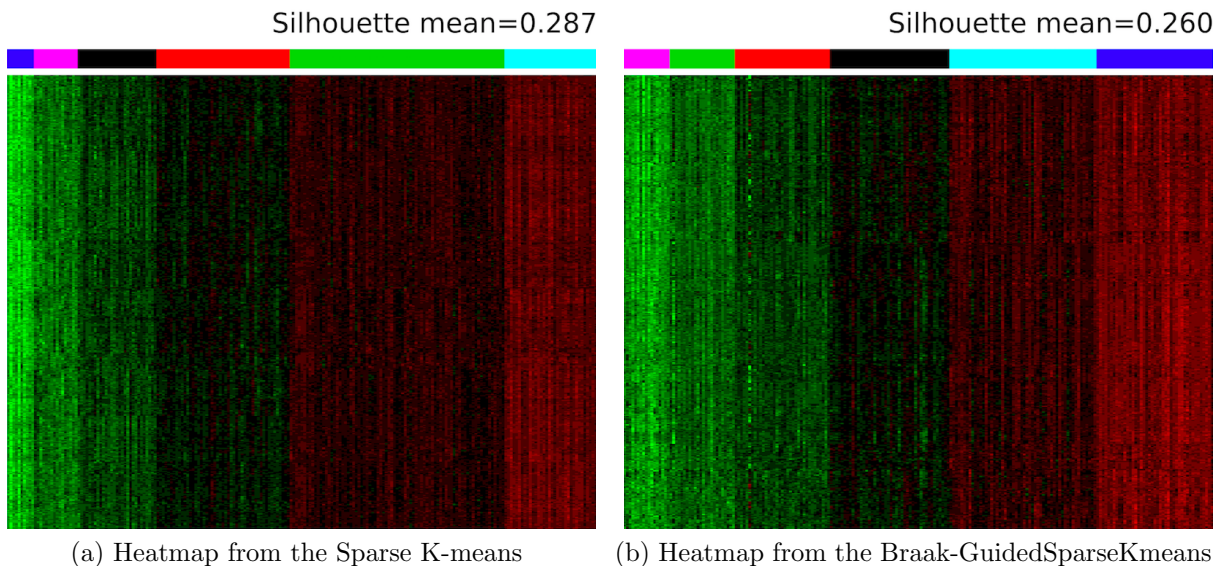


Fig. 6. Gene expression heatmap of the Alzheimer's disease dataset using the sparse K-means and the Braak-GuidedSparseKmeans. In the heatmap, rows represent genes and columns represent samples. Red color represents higher expression and green color represents lower expression. The samples are divided into 6 clusters with 6 colors in the bar above the heatmap.

5. Discussion

Since our method can only accommodate one clinical outcome variable, one issue is how to properly select the clinical guidance given multiple available clinical outcomes. We suggest to select the outcome variable of the most biological interest as clinical guidance, based on domain knowledges. Taking the Alzheimer's disease as an example, the variable Braak stage was chosen due to its important role of measuring the severity of neurofibrillary tangles in AD. If no domain knowledge can be used or one prefers a data driven approach, we suggest to try several outcome variables as guidance, and decide the best outcome guidance based on the biological interpretability of the clustering results (i.e., survival difference, pathway analysis). For example, in the breast cancer application, we would recommend the clustering result obtained by the HER2-GuidedSparseKmeans since it led to both the most significant survival difference and meaningful pathway analysis result. To further address this issue, we will develop a multivariate outcome-guided sparse K-means in the future, which will incorporate multiple outcomes variables as the clinical guidance.

In summary, we proposed an outcome-guided sparse K-means algorithm, which is capable of identifying subtype clusters via integrating clinical data with high-dimensional omics data. Our innovative methodology simultaneously solves many statistical challenges, including gene selections from high-dimensional omics data; incorporations of various types of clinical outcome variable (e.g., continuous, binary, ordinal, count or survival data) as guidance; automatic selections of tuning parameters to balance the contribution between the intrinsic genes and the clinical outcome variable; and evaluations of the relevancy of the resulting subtype clusters and the outcome variable. The superior performance of our method was demonstrated in simulations, cancer application (breast cancer gene expression data), and complicated neurodegenerative disease (Alzheimer's disease). The computing time for the GuidedSparseKmeans was fast, especially for the continuous outcome guidance, with 31 seconds for the breast cancer application with 12,180 genes and 1,870 samples, and 7 seconds for the Alzheimer's disease application with 15,363 genes and 217 samples. Our method has been implemented in R package "GuidedSparseKmeans", which is available at GitHub (<https://github.com/LingsongMeng/GuidedSparseKmeans>). With the accumulation of rich clinical data and omics data in public data repositories, we expect our innovative and fast method can be very applicable in identifying disease phenotype related subtypes.

6. Acknowledgement

L.M., D.A., and Z.H. are partially supported by NIH 2R01AI067846, G.T. is partially supported by NIH R01CA190766, R01MH111601, and R21LM012752.

References

Abramson, V. G., Lehmann, B. D., Ballinger, T. J. and Pietenpol, J. A. (2015) Subtyping of triple-negative breast cancer: Implications for therapy. *Cancer*, **121**, 8–16.

Bair, E. and Tibshirani, R. (2004) Semi-supervised methods to predict patient survival from gene expression data. *PLoS biology*, **2**, e108.

Boyd, S. and Vandenberghe, L. (2004) *Convex optimization*. Cambridge university press.

Braak, H. and Braak, E. (1991) Neuropathological stageing of alzheimer-related changes. *Acta neuropathologica*, **82**, 239–259.

Bredesen, D. E. (2015) Metabolic profiling distinguishes three subtypes of alzheimer's disease. *Aging*, **7**, 595–600.

Cox, D. and Snell, E. (1989) *Analysis of Binary Data*, vol. 32. CRC Press.

Curtis, C., Shah, S. P., Chin, S.-F., Turashvili, G., Rueda, O. M., Dunning, M. J., Speed, D., Lynch, A. G., Samarajiwa, S., Yuan, Y. et al. (2012) The genomic and transcriptomic architecture of 2,000 breast tumours reveals novel subgroups. *Nature*, **486**, 346.

Dudoit, S. and Fridlyand, J. (2002) A prediction-based resampling method for estimating the number of clusters in a dataset. *Genome Biology*, **3**, 1–21.

Efron, B. (1978) Regression and anova with zero-one data: Measures of residual variation. *Journal of the American Statistical Association*, **73**, 113–121.

Eisen, M. B., Spellman, P. T., Brown, P. O. and Botstein, D. (1998) Cluster analysis and display of genome-wide expression patterns. *Proceedings of the National Academy of Sciences*, **95**, 14863–14868.

Gaynor, S. and Bair, E. (2017) Identification of relevant subtypes via preweighted sparse clustering. *Computational statistics & data analysis*, **116**, 139–154.

Giuliano, M., Trivedi, M. V. and Schiff, R. (2013) Bidirectional crosstalk between the estrogen receptor and human epidermal growth factor receptor 2 signaling pathways in breast cancer: molecular basis and clinical implications. *Breast Care*, **8**, 256–262.

Golub, T. R., Slonim, D. K., Tamayo, P., Huard, C., Gaasenbeek, M., Mesirov, J. P., Coller, H., Loh, M. L., Downing, J. R., Caligiuri, M. A. et al. (1999) Molecular classification of cancer: class discovery and class prediction by gene expression monitoring. *science*, **286**, 531–537.

Hubert, L. and Arabie, P. (1985) Comparing partitions. *Journal of classification*, **2**, 193–218.

Huo, Z., Ding, Y., Liu, S., Oesterreich, S. and Tseng, G. (2016) Meta-analytic framework for sparse k-means to identify disease subtypes in multiple transcriptomic studies. *Journal of the American Statistical Association*, **111**, 27–42.

Huo, Z., Tseng, G. et al. (2017) Integrative sparse k -means with overlapping group lasso in genomic applications for disease subtype discovery. *The Annals of Applied Statistics*, **11**, 1011–1039.

Jaccard, P. (1901) Étude comparative de la distribution florale dans une portion des alpes et des jura. *Bull Soc Vaudoise Sci Nat*, **37**, 547–579.

Kaufman, L. and Rousseeuw, P. J. (2009) *Finding groups in data: an introduction to cluster analysis*, vol. 344. Wiley. com.

Lehmann, B. D., Bauer, J. A., Chen, X., Sanders, M. E., Chakravarthy, A. B., Shyr, Y. and Pietenpol, J. A. (2011) Identification of human triple-negative breast cancer subtypes and preclinical models for selection of targeted therapies. *The Journal of clinical investigation*, **121**, 2750.

MacQueen, J. et al. (1967) Some methods for classification and analysis of multivariate observations. In *Proceedings of the fifth Berkeley symposium on mathematical statistics and probability*, vol. 1, 281–297. Oakland, CA, USA.

McFadden, D. et al. (1977) *Quantitative methods for analyzing travel behavior of individuals: some recent developments*. Institute of Transportation Studies, University of California Berkeley.

McKelvey, R. D. and Zavoina, W. (1975) A statistical model for the analysis of ordinal level dependent variables. *Journal of mathematical sociology*, **4**, 103–120.

McLachlan, G. J., Bean, R. and Peel, D. (2002) A mixture model-based approach to the clustering of microarray expression data. *Bioinformatics*, **18**, 413–422.

Milligan, G. W. and Cooper, M. C. (1985) An examination of procedures for determining the number of clusters in a data set. *Psychometrika*, **50**, 159–179.

Nagelkerke, N. J. et al. (1991) A note on a general definition of the coefficient of determination. *Biometrika*, **78**, 691–692.

Nowak, G. and Tibshirani, R. (2008) Complementary hierarchical clustering. *Biostatistics*, **9**, 467–483.

Pan, W. and Shen, X. (2007) Penalized model-based clustering with application to variable selection. *Journal of Machine Learning Research*, **8**, 1145–1164.

Parker, J. S., Mullins, M., Cheang, M. C., Leung, S., Voduc, D., Vickery, T., Davies, S., Fauron, C., He, X., Hu, Z. et al. (2009) Supervised risk predictor of breast cancer based on intrinsic subtypes. *Journal of clinical oncology*, **27**, 1160–1167.

Parsons, D. W., Jones, S., Zhang, X., Lin, J. C.-H., Leary, R. J., Angenendt, P., Mankoo, P., Carter, H., Siu, I.-M., Gallia, G. L. et al. (2008) An integrated genomic analysis of human glioblastoma multiforme. *Science*, **321**, 1807–1812.

Paul, A. and Paul, S. (2014) The breast cancer susceptibility genes (brca) in breast and ovarian cancers. *Frontiers in bioscience (Landmark edition)*, **19**, 605.

Perou, C. M., Sørlie, T., Eisen, M. B., van de Rijn, M., Jeffrey, S. S., Rees, C. A., Pollack, J. R., Ross, D. T., Johnsen, H., Akslen, L. A. et al. (2000) Molecular portraits of human breast tumours. *Nature*, **406**, 747–752.

Prat, A., Pineda, E., Adamo, B., Galván, P., Fernández, A., Gaba, L., Díez, M., Viladot, M., Arance, A. and Muñoz, M. (2015) Clinical implications of the intrinsic molecular subtypes of breast cancer. *The Breast*, **24**, S26–S35.

Qin, Z. S. (2006) Clustering microarray gene expression data using weighted chinese restaurant process. *Bioinformatics*, **22**, 1988–1997.

Reif, A., Grünblatt, E., Herterich, S., Wichart, I., Rainer, M. K., Jungwirth, S., Danielczyk, W., Deckert, J., Tragl, K.-H., Riederer, P. et al. (2011) Association of a functional nos1 promoter repeat with alzheimer’s disease in the vita cohort. *Journal of Alzheimer’s Disease*, **23**, 327–333.

Rosenwald, A., Wright, G., Chan, W. C., Connors, J. M., Campo, E., Fisher, R. I., Gascoyne, R. D., Muller-Hermelink, H. K., Smeland, E. B., Giltnane, J. M. et al. (2002) The use of molecular profiling to predict survival after chemotherapy for diffuse large-b-cell lymphoma. *New England Journal of Medicine*, **346**, 1937–1947.

Rousseeuw, P. J. (1987) Silhouettes: a graphical aid to the interpretation and validation of cluster analysis. *Journal of computational and applied mathematics*, **20**, 53–65.

Sadanandam, A., Lyssiotis, C. A., Homicsko, K., Collisson, E. A., Gibb, W. J., Wullschleger, S., Ostos, L. C. G., Lannon, W. A., Grotzinger, C., Del Rio, M. et al. (2013) A colorectal cancer classification system that associates cellular phenotype and responses to therapy. *Nature medicine*, **19**, 619–625.

Shen, R., Olshen, A. B. and Ladanyi, M. (2009) Integrative clustering of multiple genomic data types using a joint latent variable model with application to breast and lung cancer subtype analysis. *Bioinformatics*, **25**, 2906–2912.

Song, C. and Tseng, G. C. (2014) Hypothesis setting and order statistic for robust genomic meta-analysis. *The annals of applied statistics*, **8**, 777.

Sugar, C. A. and James, G. M. (2003) Finding the number of clusters in a dataset. *Journal of the American Statistical Association*, **98**.

Tibshirani, R. and Walther, G. (2005) Cluster validation by prediction strength. *Journal of Computational and Graphical Statistics*, **14**, 511–528.

Tibshirani, R., Walther, G. and Hastie, T. (2001) Estimating the number of clusters in a data set via the gap statistic. *Journal of the Royal Statistical Society: Series B (Statistical Methodology)*, **63**, 411–423.

Tjur, T. (2009) Coefficients of determination in logistic regression models—a new proposal: The coefficient of discrimination. *The American Statistician*, **63**, 366–372.

Tothill, R. W., Tinker, A. V., George, J., Brown, R., Fox, S. B., Lade, S., Johnson, D. S., Trivett, M. K., Etemadmoghadam, D., Locandro, B. et al. (2008) Novel molecular subtypes of serous and endometrioid ovarian cancer linked to clinical outcome. *Clinical Cancer Research*, **14**, 5198–5208.

Van't Veer, L. J., Dai, H., Van De Vijver, M. J., He, Y. D., Hart, A. A., Mao, M., Peterse, H. L., Van Der Kooy, K., Marton, M. J., Witteveen, A. T. et al. (2002) Gene expression profiling predicts clinical outcome of breast cancer. *nature*, **415**, 530–536.

Verhaak, R. G., Hoadley, K. A., Purdom, E., Wang, V., Qi, Y., Wilkerson, M. D., Miller, C. R., Ding, L., Golub, T., Mesirov, J. P. et al. (2010) Integrated genomic analysis identifies clinically relevant subtypes of glioblastoma characterized by abnormalities in *PDGFRA*, *IDH1*, *EGFR*, and *NF1*. *Cancer cell*, **17**, 98–110.

Von Minckwitz, G., Untch, M., Blohmer, J.-U., Costa, S. D., Eidtmann, H., Fasching, P. A., Gerber, B., Eiermann, W., Hilfrich, J., Huober, J. et al. (2012) Definition and impact of pathologic complete response on prognosis after neoadjuvant chemotherapy in various intrinsic breast cancer subtypes. *J Clin Oncol*, **30**, 1796–1804.

Wang, B., Mezlini, A. M., Demir, F., Fiume, M., Tu, Z., Brudno, M., Haibe-Kains, B. and Goldenberg, A. (2014) Similarity network fusion for aggregating data types on a genomic scale. *Nature methods*, **11**, 333.

Wang, S. and Zhu, J. (2008) Variable selection for model-based high-dimensional clustering and its application to microarray data. *Biometrics*, **64**, 440–448.

Williams-Gray, C. H. and Barker, R. A. (2017) parkinson disease: Defining pd subtypes - a step toward personalized management? *Nature Reviews Neurology*, **13**.

Witten, D. M. and Tibshirani, R. (2010) A framework for feature selection in clustering. *Journal of the American Statistical Association*, **105**, 713–726.

Xie, B., Pan, W., Shen, X. et al. (2008) Penalized model-based clustering with cluster-specific diagonal covariance matrices and grouped variables. *Electronic Journal of Statistics*, **2**, 168–212.

Zhao, J., Deng, Y., Jiang, Z. and Qing, H. (2016) G protein-coupled receptors (gpcrs) in alzheimer's disease: a focus on bace1 related gpcrs. *Frontiers in aging neuroscience*, **8**, 58.